



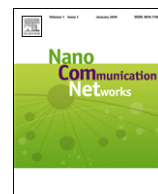
Cellular communication via directed protrusion growth: Critical length-scales and membrane morphology

Downloaded from: <https://research.chalmers.se>, 2025-12-04 22:48 UTC

Citation for the original published paper (version of record):

ZHANG, H., Kim, A., Shijun, X. et al (2015). Cellular communication via directed protrusion growth: Critical length-scales and membrane morphology. *Nano Communication Networks*, 6(4): 178-182.
<http://dx.doi.org/10.1016/j.nancom.2015.10.001>

N.B. When citing this work, cite the original published paper.



Cellular communication via directed protrusion growth: Critical length-scales and membrane morphology

Haijiang Zhang^{a,1}, Anna Kim^{a,b,1}, Shijun Xu^a, Gavin D.M. Jeffries^a, Aldo Jesorka^{a,*}

^a Department of Chemical and Biological Engineering, Chalmers University of Technology, S-412-96 Göteborg, Sweden

^b Department of Physiology and Pharmacology, Karolinska Institutet, SE-17177 Stockholm, Sweden

ARTICLE INFO

Article history:

Received 8 December 2014

Received in revised form 9 June 2015

Accepted 15 October 2015

Available online 14 November 2015

Keywords:

Cell protrusions

Cell-to-cell connections

Teflon[®] AF

Cell microgaps

Filopodia

ABSTRACT

We investigated the growth of cell protrusions from adherent HEK 293 cells and their capability to bridge cytophobic Teflon[®] AF microgaps, establishing a critical length scale, beyond which cells cannot probe free space. For this purpose, we employed a photolithography-based surface fabrication strategy for producing micropatterned substrates composed of glass and the amorphous polymer Teflon[®] AF. Cell protrusions growing from HEK 293 cells on these substrates were confined to extend on 2 μm wide glass lanes, intersected by Teflon[®] AF microgaps of various lengths between 2 and 16 μm . After 24 hours of incubation, the frequency of cell protrusions crossing the gap was found to be strongly dependent on the gap size. Gaps which are greater than 4 μm were found to be increasingly difficult to cross. Cell extensions crossing the microgaps either appeared as nanosized connections, in approximately 30% of all observed cases, or as micro-sized connections. Molecular transport in the established cell-to-cell connection across the micro-gap was investigated by activation of TRPM8 ion channels followed by supply of Ca^{2+} to one of the connected cells. The diffusion of the Ca^{2+} ions was visualized by means of a cell-permeant pre-fluorescent dye. We observed both open- and closed-ended intercellular connections in both nano- and micro-sized cell protrusions.

© 2015 The Authors. Published by Elsevier B.V. This is an open access article under the CC BY-NC-ND license (<http://creativecommons.org/licenses/by-nc-nd/4.0/>).

Introduction

Biological cells commonly migrate in response to external chemical or mechanical signals; wound healing, immune response, and tissue formation, all require the migration of cells towards specific locations. Many types of migrating cells feature filopodia, which are small, actin filament filled, plasma-membrane protrusions, typically microns in diameter [1]. One of their primary functions is to reach out from the cell, to sense and probe

their environment [1,2]. They originate from cells during migration, appearing as protrusive structures at the leading edge of a motile cell. Despite extensive studies, the biological functions of filopodia and the mechanisms of their assembly are still not fully understood. Some recent studies on filopodia function include: cellular migration and connection [1], intercellular transport and interaction [3], virus transport [4], and gene delivery [5]. Filopodia are also implicated in cancer cell motility [6]. The primary biological role of filopodia appears to be the sensing of external mechanical and chemical cues, and have been found to sense signaling molecules at large distance away from the cell body [7]. Moreover, filopodia-like structures are also implicated in cell-cell communication in invertebrates [7,8].

* Corresponding author.

E-mail address: aldo@chalmers.se (A. Jesorka).

¹ These authors contributed equally to this work.

Recently, we have demonstrated the ability to interconnect cells into a network by artificially generated nanotubes, using a micropipette assisted fabrication protocol [9]. The on-demand creation of these interconnections, facilitates the investigation of chemical species and organelle transfer between selected cells. However, our earlier investigation showed a high risk of cell damage during extrusion of cell tubes, stemming from the use of electrical pulses for membrane penetration by the glass pipette. The cells were found to reliably survive only two penetrations, which limited the possibility of generating larger cellular networks [9].

Tubular membrane interconnections have generated considerable interest, as open cell-to-cell bridges, and have been implicated in the transport of molecular cargo. The discovery of tunneling membrane nanotubes (TNTs) in 2004 as a new mode of exchange between mammalian cells [10] shed new light onto intercellular communication pathways. The formation process of TNTs between cells has previously been related to the formation of filopodia in a native cell growth environment [11,12]. Filopodia and TNTs have been found to have some structurally similar properties [13]. In this context, the possibility to generate networks of living cells, exploiting the growth and connectivity of cell protrusions would be a promising route to establish a controlled experimental environment for the study of intercellular communication.

In order to provide more insight into intercellular communication within artificial and natural cell networks, we present herein the growth of filopodia-like cell protrusions from HEK 293 adherent cells, guided by surface-fabricated microlanes. Particular focus was placed on investigating the ability of cell membrane protrusions to bridge cytophobic obstacles. Surface fabrication and cell culture protocols were established; and chemical transport through the established tubular connections was evaluated using interconnected pairs of cells.

In our experimental study, we directed the growth of cell protrusions in cytophobic Teflon® AF-framed glass microstructures, featuring 2 μm wide glass lanes intersected by a Teflon® AF microgap of varying lengths, from 2 μm to 16 μm (Supplementary Information S1). Teflon® AF (amorphous copolymer of polytetrafluoroethylene (PTFE) with 2,2-bis(trifluoromethyl)-4,5-difluoro-1,3-dioxole) is typically chosen as the surface coating material, as it features strong hydrophobicity, high gas permeability [14] and has very low autofluorescence, which is of key importance for fluorescence microscopy imaging. One major benefit of Teflon AF, as opposed to other surface mediated growth strategies [15], rendering it particularly suitable for our study, is its ability to guide cell growth, due to its cytophobic, but not cytotoxic, properties [16]. An optimized variant of a previously reported micropatterning technique was employed to produce Teflon® AF-framed glass microstructures [17], which were appropriately sized to accommodate up to three HEK 293 cells per circular region. Other examples of micropatterned surfaces for the study of filopodia-like cell protrusions exist [18–20], but none of them exploit the specific properties of Teflon® AF to guide growth while minimizing cell adhesion to undesired binding events.

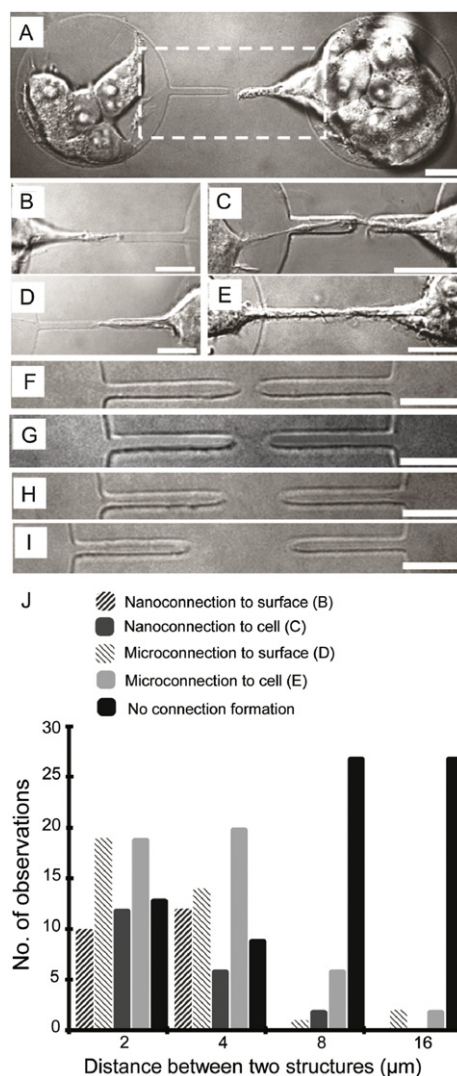


Fig. 1. Teflon® AF patterned glass cover slip and intercellular tubular growth. (A) Cell adhesion to the circular glass surface and filopodia-like protrusion growth along the Teflon-framed lane. (B–E) Bright-field images of the identified types of intercellular connections for microgaps of different length. (B) Image of a cell forming a nanosized bridge head to the glass surface across a microgap. (C) Image of a cell forming a nanoconnection with another cell across a microgap. (D) Image of a cell forming a micro-sized bridgehead to the glass surface across a microgap. (E) Image of a cell forming a microconnection with another cell across a microgap. (F–I) Images of various microgap separations between two structures (2, 4, 8 and 16 μm long, respectively). (J) A graph summarizing the total number of the different types of intercellular connections observed for different microgap lengths. The scale bars in panels A–I represent 10 μm .

On the micropatterned surfaces, cells directly adhere and grow on the exposed glass regions, where the development of cell protrusions along the Teflon® AF-framed lanes could be observed (Fig. 1(A)–(E)). We incorporated various Teflon® AF gap junction distances in the glass lanes (Fig. 1(F)–(I)), and fabricated them in large areas on each surface to enable many patterning variants to be present on each micropatterned surface (Supplementary Information Figure S2). Since this cytophobic gap does not support cell adhesion, the ability of the approaching mem-

brane structure to form a bridge across the junction could be evaluated. We determined the influence of the junction distance on the ability to form interconnections between protrusions originating from two adjacent cells. We separated the protrusions based upon characteristics of interconnections in the submicrometer (nanoconnection) and micrometer (microconnection) ranges, while bridging the microgap (Fig. 1(J)). We also determined if the interconnections formed, were closed (junctions) or open (tunnels) to the exchange of ions and molecules, revealing that in some cases, the cell protrusions can support molecular transport.

Results

Glass coverslips with micropatterned Teflon[®] AF were fabricated utilizing photolithography and lift-off procedures (Supplementary Information S1). The microstructures, revealing areas of glass on the surface, feature a circular area of 50 μm connected to a 20 μm long and 2 μm width lane, surrounded by Teflon[®] AF. The gap junction distances separating one microstructure from another, were designed to be 2, 4, 8 and 16 μm , presented in Fig. 1(F)–(I). The microgap spacing was chosen to be 2, 4, 8 and 16 μm , to span a broad range of cellular size scales, while staying within the fidelity of the fabrication protocols: 2 and 4 μm being representative of local phenomenon, comfortably smaller than cell width dimensions, 8 μm to represent approximately the cell width, 16 μm to be a longer distance than the width of most single cells. HEK 293 cells were cultured for two days on patterned surfaces (Supplementary Information S2 and S3), together with a membrane dye (0.001 mg/mL deep red plasma membrane stain—CellMask). After incubation the HEK 293 cells adhered to the exposed glass regions and cell protrusions began to grow along the surface and the lane, as in Fig. 1(A). After the front of the protrusion reached the Teflon[®] AF microgap, we observed two types of behavior: (1) halting of the protrusion propagation, or (2) bridging of the Teflon[®] AF microgap (Supplementary Information S4). Confocal microscopy was performed on a Leica TCS SP 2 instrument and a 649 nm Ar^+ laser was used for excitation of membrane dye (Supplementary Information S5).

The analysis of the occurrence of bridge formation over the microgap, with respect to the gap separation, is presented in Fig. 1(J). The microgaps with a length of 2 and 4 μm appeared to be grown over by the cell protrusions more readily than the gaps ranging in size between 8 and 16 μm . In only a few instances junction distances greater than 8 μm could be bridged. Given the short distance, and the cytophobicity of the gap material, we hypothesize that the formation and growth of nanoconnections are a possible pathway assumed by the cells, to bridge the junction distance. A TNT-like nanoconnection could be formed from the free end of the growing protrusion, extend across the Teflon[®] AF gap without adhesion, and connect to the glass substrate on the opposite side of the gap (Fig. 1(B)). This would imply that such nanoconnections could aid filopodia-like protrusions in successfully bridging obstacles. The diameter of the fully formed intercellular nanoconnection at the microgap was measured as ~ 0.5 to 0.9 μm in Fig. 1(C), which is

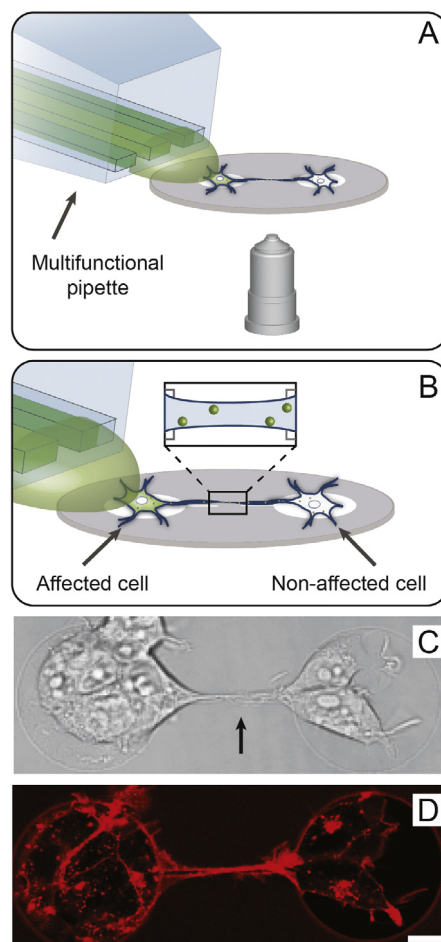


Fig. 2. Cell-to-cell molecular transport through tubular interconnections, via selected cell superfusion. (A–B) Schematic drawing of the multifunctional pipette used in the experiments to expose only one of the connected cells. (C–D) Confocal images of cells interconnected by a nano-sized connection. The images were obtained from the sets of experiments used for observing molecular transport and its time scale across such connections. (C) Bright-field image of the cells. The black arrow in the figure marks the position of the 2 μm Teflon[®] AF microgap. The multifunctional pipette was positioned on top of the cells located on the left-hand side. (D) Confocal image of the cells with a red membrane staining dye (CellMask) to verify microgap bridging. The scale bar is 10 μm . (For interpretation of the references to color in this figure legend, the reader is referred to the web version of this article.)

considerably less than the dimensions of the gap-bridging and intercellular microconnections in Fig. 1(D) and (E).

The cell protrusions that span the microgaps were subsequently evaluated in terms of their ability to transport molecular cargo. HEK 293 cells, expressing the ion channel TRPM8, were plated and stained with CellMask deep red cell membrane stain. Directly prior to experimentation, the plated cells were incubated with Calcium green-1 dye, an intracellular fluorescent indicator dye, capable of sensing changes of calcium concentration. The multifunctional pipette, a hydrodynamically confined microflow device [21], was then utilized to selectively expose one of the connected cells with 50 μM Menthol (for activation of TRPM8 ion channels), in the presence of a 10 mM Ca^{2+} spiked buffer solution (Fig. 2) (Supplementary

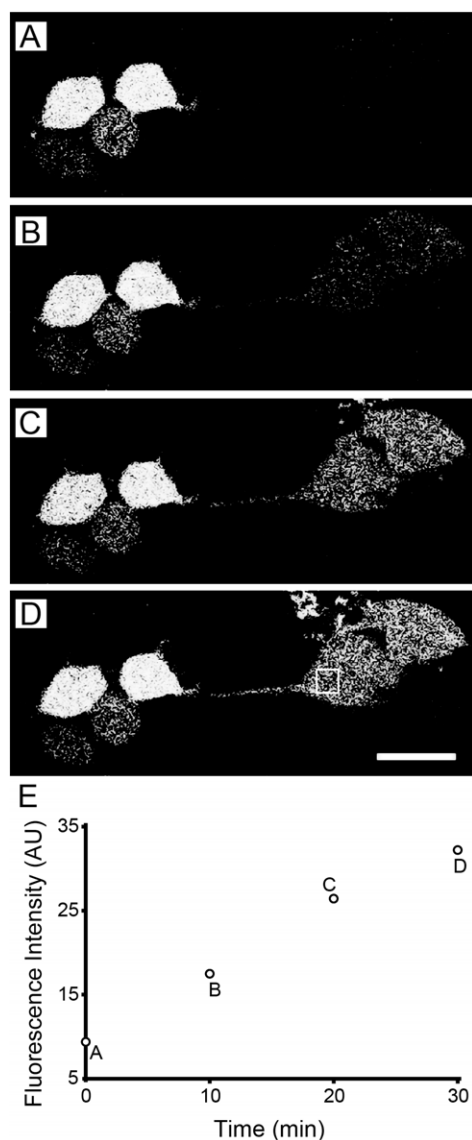


Fig. 3. Diffusive transport of Ca^{2+} through an intercellular nanoconnection. (A–D) Confocal time series of molecular transport through the intercellular connection. The regions of interest (ROI) is indicated by the square in (D). The corresponding intensity vs. time curve in (E) shows the change of the fluorescence signal in the target cell. The scale bar represents 10 μm .

Information S6). The transport of Ca^{2+} ions from one cell to the other was then monitored through the interconnection across a microgap, by monitoring the change of fluorescent intensity of the non-exposed cell. (Fig. 3(A)–(D)). The average diffusion time between the cells through a nanoconnection was 30 min and 35 s for a microconnection (Supplementary Information S6). The diffusion time, as expected, was found to be significantly dependent on the diameter of the connection, and the observed time scale for molecular transport in a microconnection was found to be approximately 50 times faster than in a nanoconnection. During data collection, both open (tunnel) and closed (junction) interconnections, were found to occur.

Conclusion

We investigated the effect of a cytophobic microgap and its dimensions on the formation of intercellular connections, demonstrating the extent to which cells can effectively probe and span the surrounding space. Subsequently we examined the ability of these formed connections to transport molecular cargo. We found that molecular diffusion can occur through both nano- and microconnections, across the cytophobic microgaps, providing evidence that these connections may have some transport functions similar to TNTs. We successfully established a new experimental platform for the on-demand generation of interconnections between adherent cells, which can significantly facilitate investigations of molecular transport phenomenon in artificial cellular networks. We have shown that two cells can be interconnected by an appropriately designed surface, which we expect can be extended, through lane and gap complexity, to larger networks. In this context, we also expanded and optimized our previously reported fabrication procedure for microstructures in Teflon[®] AF on glass substrates, for shorter length scale investigations. Our findings provide new experimental opportunities for the investigation of cellular communication, and address the growing demand for new technologies for single-cell analysis.

Acknowledgments

This work was made possible through financial support obtained from the European Research Council (Horizon 2020 project # 664786), Vetenskapsrådet (VR), Nordforsk, and the Chalmers Area of Advance in Nanoscience and Technology.

Appendix A. Supplementary data

Supplementary material related to this article can be found online at <http://dx.doi.org/10.1016/j.nancom.2015.10.001>. It includes details on surface fabrication, cell culturing, and statistics. Additional experimental results are also provided.

References

- [1] P.K. Mattila, P. Lappalainen, Filopodia: molecular architecture and cellular functions, *Nat. Rev. Mol. Cell Biol.* 9 (6) (2008) 446–454.
- [2] D. Hanein, P. Matsudaira, D.J. DeRosier, Evidence for a conformational change in actin induced by fimbrin (N375) binding, *J. Cell Biol.* 139 (2) (1997) 387–396.
- [3] P.I. Zhuravlev, et al., Theory of active transport in filopodia and stereocilia, *Proc. Natl. Acad. Sci. USA* 109 (27) (2012) 10849–10854.
- [4] M.J. Lehmann, et al., Actin- and myosin-driven movement of viruses along filopodia precedes their entry into cells, *J. Cell Biol.* 170 (2) (2005) 317–325.
- [5] Z.U. Rehman, et al., Nonviral gene delivery vectors use syndecan-dependent transport mechanisms in filopodia to reach the cell surface, *ACS Nano* 6 (8) (2012) 7521–7532.
- [6] A. Arjonen, R. Kaukonen, J. Ivaska, Filopodia and adhesion in cancer cell motility, *Cell Adhesion Migr.* 5 (5) (2011) 421–430.
- [7] T. Bornschlöggl, How filopodia pull: What we know about the mechanics and dynamics of filopodia, *Cytoskeleton* 70 (10) (2013) 590–603.

- [8] F.-A. Ramírez-Weber, T.B. Kornberg, Cytonemes: Cellular processes that project to the principal signaling center in drosophila imaginal discs, *Cell* 97 (5) (1999) 599–607.
- [9] H. Zhang, et al., Artificial nanotube connections and transport of molecular Cargo between mammalian cells, *Nano Commun. Netw.* 4 (4) (2013) 197–204.
- [10] A. Rustom, et al., Nanotubular highways for intercellular organelle transport, *Science* 303 (5660) (2004) 1007–1010.
- [11] H.H. Gerdes, A. Rustom, Tunneling nanotubes: Membranous channels between animal cells, in: Frantisek Baluska, Dieter Volkmann, Peter W. Barlow (Eds.), *Cell-Cell Channels*, 2006 (Chapter 14).
- [12] E.A. Eugenin, P.J. Gaskill, J.W. Berman, Tunneling nanotubes (TNT) are induced by HIV-infection of macrophages: A potential mechanism for intercellular HIV trafficking, *Cell. Immunol.* 254 (2) (2009) 142–148.
- [13] N.M. Sherer, et al., Retroviruses can establish filopodial bridges for efficient cell-to-cell transmission, *Nat. Cell Biol.* 9 (3) (2007) 310–315.
- [14] I. Pinnau, L.G. Toy, Gas and vapor transport properties of amorphous perfluorinated copolymer membranes based on 2,2-bis(trifluoromethyl)-4,5-difluoro-1,3-dioxole/tetrafluoroethylene, *J. Membr. Sci.* 109 (1) (1996) 125–133.
- [15] C.H. Thomas, et al., Surfaces designed to control the projected area and shape of individual cells, *J. Biomech. Eng.* 121 (1) (1999) 40–48.
- [16] S.A. Makohliso, et al., Application of teflon-AF thin films for biopatterning of neural cell adhesion, *Biosens. Bioelectron.* 13 (11) (1998) 1227–1235.
- [17] I. Czolkos, et al., High-resolution micropatterned teflon AF substrates for biocompatible nanofluidic devices, *Langmuir* 28 (6) (2012) 3200–3205.
- [18] J. Albuschies, V. Vogel, The role of filopodia in the recognition of nanotopographies, *Sci. Rep.* 3 (2013) 1658.
- [19] M.J. Dalby, et al., Investigating filopodia sensing using arrays of defined nano-pits down to 35 nm diameter in size, *Int. J. Biochem. Cell Biol.* 36 (10) (2004) 2005–2015.
- [20] K.J. Jang, et al., Two distinct filopodia populations at the growth cone allow to sense nanotopographical extracellular matrix cues to guide neurite outgrowth, *PLoS One* 5 (12) (2010).
- [21] A. Ainla, et al., A multifunctional pipette, *Lab Chip* 12 (7) (2012) 1255–1261.



Haijiang Zhang received his M.Sc. in Biotechnology from Chalmers University of Technology in 2009, and started his Ph.D. research in the Biophysical Chemistry group of Prof. Owe Orwar in the same year. In 2013, he received his Ph.D. degree in Bionanotechnology and Biophysical Chemistry.



Anna Kim received her M.Sc. in Materials and Nanotechnology from Chalmers University of Technology (Sweden) in 2012. Currently, she is completing her Ph.D. at the same university in collaboration with Karolinska Institute (Sweden). Her research focus is on the development of microtechnologies as a scientific tool for biological applications.



Shijun Xu is a technical consultant at Nanjing Haifu Medical Technology Co. Ltd. She received her M.Sc. (2010) and Ph.D. (2014) in Biophysical Chemistry at Chalmers University of Technology in Sweden. Her research is focused on new technologies for single cell research.



Gavin D.M. Jeffries received his Ph.D. degree in Chemistry from the University of Washington, Seattle, in 2008. He received a M.Chem. from the University of York in 2002. He is currently an assistant professor in the Chemical Engineering Department of Chalmers University of Technology, where his research interests are centered around single-cell analysis, with emphasis on technological development to study inter- and intra-cellular communication.



Aldo Jesorka did his undergraduate research in Chemistry at Leipzig University and the University of Florida from 1989–1994. After spending an exchange year at the RIKEN institute in Tokyo, Japan, he commenced research at the Max Planck Institute for Radiation Chemistry/Germany in 1996. After graduation with a doctorate in Natural Sciences in 2000, he performed postdoctoral work at Arizona State University. He then moved to Chalmers University of Technology in Sweden, where he became senior research scientist in 2004 and associate professor in 2009. He is the head of the Biophysical Technology Laboratory at Chalmers since 2011, where he is active in the field of integrative micro- and nanosciences.